

NEW LOW-MASS MEMBERS OF THE TAURUS STAR-FORMING REGION¹

K. L. LUHMAN,² CÉSAR BRICEÑO,³ JOHN R. STAUFFER,⁴ LEE HARTMANN,⁵
D. BARRADO Y NAVASCUÉS,⁶ AND NELSON CALDWELL⁷

Received 2003 January 16; accepted 2003 February 25

ABSTRACT

Briceño et al. recently used optical imaging, data from the Two-Micron All-Sky Survey (2MASS), and follow-up spectroscopy to search for young low-mass stars and brown dwarfs in 8 deg² of the Taurus star-forming region. By the end of that study, there remained candidate members of Taurus that lacked the spectroscopic observations needed to measure spectral types and determine membership. In this work, we have obtained spectroscopy of the 22 candidates that have $A_V \leq 8$, from which we find six new Taurus members with spectral types of M2.75 through M9. The new M9 source has the second latest spectral type of the known members of Taurus ($\sim 0.02 M_\odot$). Its spectrum contains extremely strong emission in H α ($\lambda \sim 950 \text{ \AA}$), as well as emission in He I 6678 Å and the Ca II IR triplet. This is the least massive object known to exhibit emission in He I and Ca II, which together with the strong H α are suggestive of intense accretion.

Subject headings: infrared: stars — stars: evolution — stars: formation —
stars: low-mass, brown dwarfs — stars: luminosity function, mass function —
stars: pre-main-sequence

1. INTRODUCTION

Magnitude-limited searches for members of nearby star-forming regions are an important basis for a variety of studies of young stars and brown dwarfs. For instance, such surveys provide well-defined membership samples from which unbiased initial mass functions (IMFs) can be derived. In addition, newly discovered young brown dwarfs are valuable targets for detailed studies of the formation of objects at the bottom of the mass function.

The Taurus dark cloud complex has proven to be amenable to a census of its low-mass stars and brown dwarfs. The members of this region are nearby (140 pc) and young (1 Myr) and thus can be detected down to very low masses. In addition, because a majority of the members of Taurus (excluding protostars) exhibit relatively low extinction ($A_V \lesssim 5$), they are accessible to measurements at both optical and infrared (IR) wavelengths. Over time, surveys for new members in this low-density, dispersed population ($n \sim 1\text{--}10 \text{ pc}^{-3}$) have steadily expanded in areal coverage (Strom & Strom 1994; Briceño et al. 1998; Luhman & Rieke

1998; Luhman 2000; Martín et al. 2001). Most recently, Briceño et al. (2002) used wide-field optical imaging, Two-Micron All-Sky Survey (2MASS) data, and follow-up spectroscopy to search for low-mass stars and brown dwarfs in 8 deg² that encompassed half of the known pre-main-sequence population in Taurus. They discovered nine new members with spectral types of M5.75–M9.5, corresponding to masses of 0.1–0.015 M_\odot by the theoretical evolutionary models of Baraffe et al. (1998).

At the conclusion of the study by Briceño et al. (2002), there remained candidate members of Taurus that had not been observed spectroscopically. In this paper, we identify the most promising of those candidates (§ 2), describe spectroscopic observations of them (§ 3), measure spectral types and determine whether they are Taurus members (§ 4), and discuss the physical properties of the six new members and update the IMF from Briceño et al. (2002) (§ 5).

2. SELECTION OF CANDIDATE MEMBERS OF TAURUS

Briceño et al. (2002) used optical and near-IR photometry to select potential young stars and brown dwarfs in 8 deg² of Taurus. In this section, we examine the photometry from that survey to identify the remaining candidates that lack the spectroscopy needed to confirm membership in Taurus and to measure spectral types. To do this, we could simply use the observed color-magnitude and color-color diagrams (e.g., I vs. $I-Z$, $J-H$ vs. $I-K_s$) in the manner described by Briceño et al. (2002). Instead, we revise those methods in a way that more clearly separates Taurus members from field stars.

We wish to identify the stars in the fields surveyed by Briceño et al. (2002) that have both the colors and the absolute photometry expected of members of the Taurus population. Optical color-magnitude diagrams (CMDs) are widely used for selecting candidate members of clusters on this basis. However, in star-forming clouds, the presence of

¹ Based on observations obtained at the Kitt Peak National Observatory, Keck Observatory, Fred Lawrence Whipple Observatory, and the MMT Observatory. This publication makes use of data products from the Two Micron All Sky Survey, which is a joint project of the University of Massachusetts and the Infrared Processing and Analysis Center/California Institute of Technology, funded by the National Aeronautics and Space Administration and the National Science Foundation.

² Harvard-Smithsonian Center for Astrophysics, 60 Garden Street, Cambridge, MA 02138; kluhman@cfa.harvard.edu.

³ Centro de Investigaciones de Astronomía, Apartado Postal 264, Mérida 5101-A, Venezuela; briceno@cida.ve.

⁴ SIRT Science Center, Caltech MS 314-6, Pasadena, CA 91125; stauffer@ipac.caltech.edu.

⁵ Harvard-Smithsonian Center for Astrophysics, 60 Garden Street, Cambridge, MA 02138; lhartmann@cfa.harvard.edu.

⁶ Laboratorio de Astrofísica Espacial y Física Fundamental, INTA, P.O. Box 50727, 28080 Madrid, Spain; barrado@laeff.esa.es.

⁷ Harvard-Smithsonian Center for Astrophysics, 60 Garden Street, Cambridge, MA 02138; ncaldwell@cfa.harvard.edu.

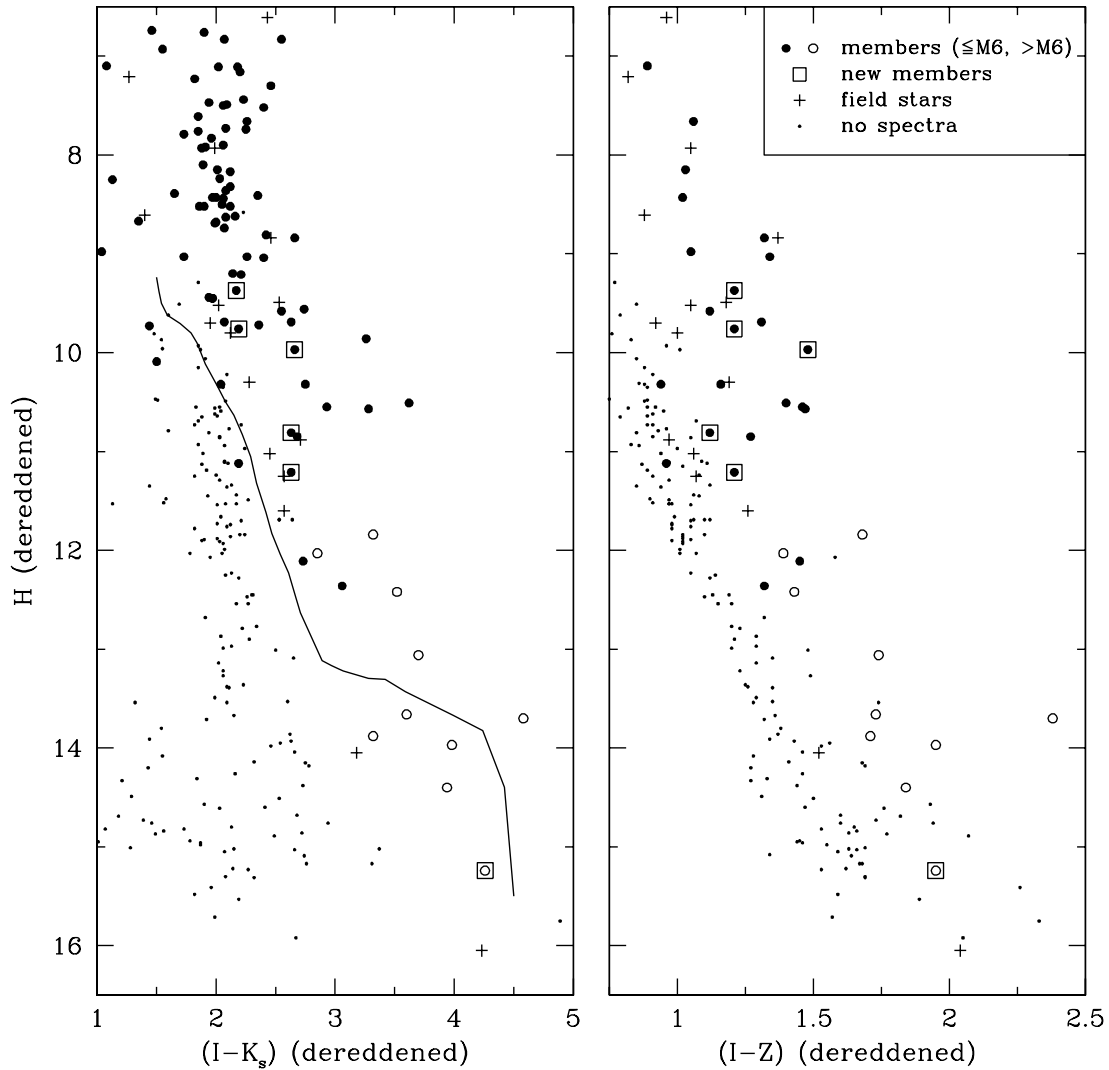


FIG. 1.—Extinction-corrected color-magnitude diagrams for stars with $A_V \leq 8$ in the 8 deg^2 surveyed by Briceño et al. (2002) in the Taurus star-forming region. We plot the stars that have been spectroscopically confirmed as Taurus members at $\leq M6$ and $>M6$ (filled and open circles, respectively) and indicate the ones found in this work (boxes). Members later than M6 are likely to be brown dwarfs by the H-R diagram and evolutionary models in Fig. 5. The field stars identified in this study are also shown (plus signs). The remaining stars lack spectra (points). The solid line is the 10 Myr isochrone ($1-0.015 M_\odot$) from the evolutionary models of Baraffe et al. (1998). The members below the isochrone at $H = 9.5-11.5$ are known or suspected to be seen in scattered light (Briceño et al. 2002).

highly variable extinction ($A_V = 0-20$ in Taurus) increases the contamination of background stars in the region of the CMD inhabited by members and prevents reliable mass estimates for candidate members (i.e., reddened high-mass members and unreddened low-mass members can have the same optical color and magnitude). The photometry in such diagrams cannot be corrected for extinction when only two bands are available. In the case of the Taurus fields, in addition to I and Z photometry, we have near-IR data from 2MASS. As a result, we have been able to estimate the extinction toward each star by dereddening its position in $J-H$ versus $I-K_s$ until it intersects the sequence of colors for dwarfs later than K6 (Leggett 1992), which is the range of spectral types occupied by most known members of Taurus. If a star has a spectral type earlier than K6, the extinction will be underestimated in this method, but that is acceptable. The dereddening process tends to remove background stars from the area of the CMD where members reside, and if a star's extinction is underestimated, then at

worst it remains in that area and is selected as a candidate. In other words, an underestimate of extinction will not result in the rejection of a bona fide member. After correcting the photometry for extinction in this way, we plot the results on CMDs of $I-K_s$ versus H and $I-Z$ versus H in Figure 1. We choose H as the magnitude because it correlates closely with bolometric luminosity, requires only a small correction for extinction, and is not susceptible to significant contamination from excess emission from circumstellar material. Meanwhile, the $I-K_s$ and $I-Z$ colors are used because they increase rapidly with decreasing mass, producing a member sequence that is distinct from the location of most field stars in the CMDs. In Figure 1, we omit the stars appearing below the reddening vector in the diagram of I versus $I-Z$ in Briceño et al. (2002) because they are well below the member sequence and are thus likely to be field stars. From the ~ 250 stars that remain, we plot only those that exhibit extinctions of $A_V \leq 8$. We are primarily interested in identifying candidate members at lower extinctions

TABLE 1
BACKGROUND STARS

2MASSs	α (J2000) ^a	δ (J2000) ^a	Spectral Type	I^b	$I-Z^b$	$J-H^a$	$H-K_s^a$	K_s^a
J0413179+281143.....	04 13 17.97	28 11 43.0	Giant	14.55	1.42	1.19	0.49	10.22
J0417519+282551.....	04 17 51.94	28 25 51.1	Giant	15.37	1.39	1.04	0.56	11.18
J0418021+281748.....	04 18 02.15	28 17 48.9	M2-M4 V	19.49	1.93	1.12	0.80	14.13
J0418053+282801.....	04 18 05.38	28 28 01.3	Giant	16.08	1.75	1.59	0.72	10.33
J0418423+281140.....	04 18 42.38	28 11 40.7	Giant	12.01	1.22	0.65	0.29	9.28
J0419273+281301.....	04 19 27.37	28 13 01.1	Giant	13.11	1.51	1.55	0.55	8.16
J0426255+260653.....	04 26 25.50	26 06 53.4	Giant	15.46	1.28	1.00	0.48	11.08
J0426344+260740.....	04 26 34.45	26 07 40.2	Giant	15.85	1.72	1.32	0.70	10.75
J0427428+262256.....	04 27 42.87	26 22 56.7	Giant	13.02	1.57	1.42	0.61	7.33
J0432113+261323.....	04 32 11.33	26 13 23.6	Giant	13.64	1.73	1.09	0.40	9.24
J0432138+263046.....	04 32 13.82	26 30 46.1	Giant	13.33	1.38	1.30	0.45	9.25
J0433080+255643.....	04 33 08.03	25 56 43.7	Giant	13.97	1.67	1.49	0.61	8.67
J0433293+261809.....	04 33 29.33	26 18 09.6	Giant	15.10	1.45	1.38	0.58	10.29
J0433341+181426.....	04 33 34.11	18 14 26.2	Giant	15.13	1.29	0.89	0.34	11.39
J0433513+262614.....	04 33 51.33	26 26 14.3	Early	16.58	1.67	1.14	0.65	11.84
J0436008+225517.....	04 36 00.85	22 55 17.4	M7 V \pm 0.5	19.92	2.04	0.60	0.37	15.69

NOTE.—Units of right ascension are hours, minutes, and seconds, and units of declination are degrees, arcminutes, and arcseconds.

^a 2MASS Spring 1999 Release Point Source Catalog.

^b Briceño et al. 2002.

that might fall within the limit of $A_V \leq 4$ that defined the IMF from Briceño et al. (2002) so that we can approach 100% completeness for that sample. The extinctions derived for the construction of Figure 1 are only rough estimates since they are based on photometry alone without any information on the spectral types. Therefore, to be certain that members at $A_V \leq 4$ were not missed, we considered a threshold of $A_V \leq 8$ in selecting candidates. In Figure 1, we include all objects that have been spectroscopically confirmed as members in this work and in previous studies for the Taurus fields in question. We also indicate the field stars identified through our new spectroscopy, while omitting the field stars found in previous work.

We now describe the regions in Figure 1 that are inhabited by Taurus members and examine the photometry to identify any potential members that lack previous spectra. When the known members of Taurus are placed on a Hertzsprung-Russell ($H-R$) diagram, they exhibit median and maximum ages of ~ 1 and 10 Myr, respectively, on the model isochrones of Baraffe et al. (1998), except at the latest spectral types, where some of the members appear between the isochrones for 10 and 30 Myr (Briceño et al. 2002; § 5.2). We plot the 10 Myr isochrone from 0.015 to 1 M_\odot in the diagram of $I-K_s$ versus H in Figure 1 by combining the predicted effective temperatures and bolometric luminosities (Baraffe et al. 1998), a temperature scale that is compatible with the adopted models (Luhman 1999; Luhman et al. 2003), dwarf colors and bolometric corrections (Leggett 1992; Luhman 1999), and a distance modulus of 5.76 (Wichmann et al. 1998). The plateau near $H = 13.5$ in the resulting isochrone in Figure 1, which does not appear in a plot of the isochrone in T_{eff} versus L_{bol} , reflects the rapid increase in $I-K_s$ between M5 and M9. Because standard values of intrinsic $I-Z$ as a function of spectral type are not available, we cannot plot the isochrone in $I-Z$ versus H . However, the lower envelope of the sequence of known members in $I-Z$ versus H effectively delineates the location of the 10 Myr isochrone (except at late types, or $I-Z > 1.7$) and the line above which we should search for new

members. Approximately 23 stars lack spectra and fall near the member sequences in both of the CMDs in Figure 1. In the next section, we describe spectroscopy of 22 of these stars, which are listed in Tables 1 and 2. The remaining source is 2MASSs 0435283+241000, which has dereddened photometry of $H = 15.75$, $I-Z = 2.33$, and $I-K_s = 4.89$. We did not observe this star because it is at the detection limits of both the optical and 2MASSs data and therefore its positions in the CMDs are highly uncertain.

3. SPECTROSCOPIC OBSERVATIONS OF CANDIDATES

Table 3 summarizes our observations of the 22 candidate members of Taurus identified in the previous section. One of these objects, 2MASSs J0419012+280248, was observed on two occasions. The FAST spectrometer (Fabricant et al. 1998) on the 1.5 m Tillinghast reflector at the Fred Lawrence Whipple Observatory was operated with the 300 line mm^{-1} grating ($\lambda_{\text{blaze}} = 4800 \text{ \AA}$) and 2'' slit, providing a resolution of $\text{FWHM} = 5 \text{ \AA}$. The Keck I low-resolution imaging spectrometer (LRIS; Oke et al. 1995) was configured with the 400 line mm^{-1} grating ($\lambda_{\text{blaze}} = 8500 \text{ \AA}$), GG495 blocking filter, and 1'' slit ($\text{FWHM} = 6 \text{ \AA}$). With the Blue Channel spectrometer at the MMT Observatory, we used the 600 line mm^{-1} grating ($\lambda_{\text{blaze}} = 9630 \text{ \AA}$), LP495 blocking filter, and 1'' slit ($\text{FWHM} = 2.7 \text{ \AA}$). Each spectrum was collected with the slit rotated to the parallactic angle. The exposure times ranged from 300 to 2700 s. After bias subtraction and flat-fielding, the spectra were extracted and calibrated in wavelength with arc lamp data. The spectra were then corrected for the sensitivity functions of the detectors, which were measured from observations of spectrophotometric standard stars.

4. SPECTRAL CLASSIFICATION OF CANDIDATES

We measure spectral types and assess membership for the 22 candidate Taurus members that were observed spectroscopically by applying the methods of classification

TABLE 2
NEW MEMBERS OF TAURUS

ID	2MASSs ID	$\alpha(J2000)^a$	$\delta(J2000)^a$	Spectral Type/ W_λ (H α)	T_{eff}^b	A_J	L_{bol}	I^c	$I-Z^c$	$J-H^a$	$H-K_s^a$	K_s^a
KPNO-Tau 10	J0417495+281331	04 17 49.54	28 13 32.0	M5 \pm 0.25 / 36 \pm 5	3125	0.14	0.052	13.94	1.25	0.77	0.32	10.78
KPNO-Tau 11	J0418302+274320	04 18 30.30	27 43 20.6	M5.5 \pm 0.25 / 14 \pm 1	3058	0.00	0.049	13.72	1.22	0.61	0.23	11.01
KPNO-Tau 12	J0419012+280248	04 19 01.26	28 02 48.7	M9 \pm 0.25 / 950 \pm 100	2400	0.14	0.00082	19.69	2.04	0.82	0.50	14.94
KPNO-Tau 13	J0426573+260628	04 26 57.31	26 06 28.8	M5 \pm 0.25 / 10 \pm 1	3125	0.70	0.15	13.70	1.57	1.11	0.56	9.60
KPNO-Tau 14	J0433078+261606	04 33 07.81	26 16 06.6	M6 \pm 0.25 / 40 \pm 10	2990	0.85	0.11	14.98	1.86	1.10	0.54	10.27
KPNO-Tau 15	J0435510+225240	04 35 51.10	22 52 40.1	M2.75 \pm 0.25 / 5.8 \pm 0.5	3451	0.56	0.14	13.63	1.48	0.98	0.33	10.01

^a 2MASS Spring 1999 Release Point Source Catalog.

^b Temperature scale of Luhman et al. 2003.

^c Briceño et al. 2002.

TABLE 3
OBSERVING LOG

Date	Telescope + Instrument	2MASSs
2002 Jan 12	MMT + Blue Channel	J0419012+280248
2002 Sep 12	FLWO 1.5 m + FAST	J0418423+281140
		J0432113+261323
		J0435510+225240
		J0418302+274320
2002 Sep 27	FLWO 1.5 m + FAST	J0417495+281331
2002 Nov 5	Keck + LRIS	J0436008+225517
		J0419012+280248
2002 Nov 10	MMT + Blue Channel	J0418021+281748
2002 Dec 7	FLWO 1.5 m + FAST	J0413179+281143
		J0426573+260628
		J0432138+263046
		J0433078+261606
		J0433080+255643
2002 Dec 14	MMT + Blue Channel	J0419273+281301
		J0426344+260740
		J0427428+262256
		J0433293+261809
		J0433513+262614
2002 Dec 15	MMT + Blue Channel	J0417519+282551
		J0418053+282801
		J0426255+260653
		J0433341+181426

described in our previous studies of Taurus and other young populations (Luhman 1999; Briceño et al. 2002).

We classify 13 candidates as background giants and one candidate as a background early-type star. Strong absorption in the Ca II triplet is the most distinguishing feature of the giants, as illustrated for two of these stars in Figure 2.

The data for the other eight candidates are displayed in Figure 2. Two of these stars, 2MASSs J0418021+281748 and J0436008+225517, are below the main sequence when placed on the H-R diagram with the distance of Taurus, which indicates that they are probably field dwarfs behind the star-forming region. Although young stars that are observed in scattered light can appear at comparable positions on the H-R diagram (Briceño et al. 2002; § 5.2), such stars usually exhibit emission in H α or some other evidence of youth. However, no such signatures are found in the data for these two stars. In addition, the strength of the K I and Na I absorption in the spectrum of 2MASSs J0436008+225517 provides conclusive evidence that it is a field dwarf.

The spectra for the six remaining sources in Figure 2 exhibit evidence of youth—and thus membership in Taurus—in the form of the weak K I and Na I absorption features that are characteristic of pre-main-sequence objects (Martín et al. 1996; Luhman et al. 1998a, 1998b; Luhman 1999). The membership of five of these sources is independently established by the presence of reddening in their spectra and their positions above the main sequence for the distance of Taurus, which indicate that they cannot be field dwarfs in the foreground or the background of the cloud, respectively. The equivalent widths of H α emission in KPNO-Tau 11, 13, and 15 are consistent with those of both active field dwarfs and young objects. Meanwhile, the much stronger emission in KPNO-Tau 10, 12, and 14 is common among the latter but rare in the former (Gizis et al. 2000). For the coolest new member, KPNO-Tau 12, we find

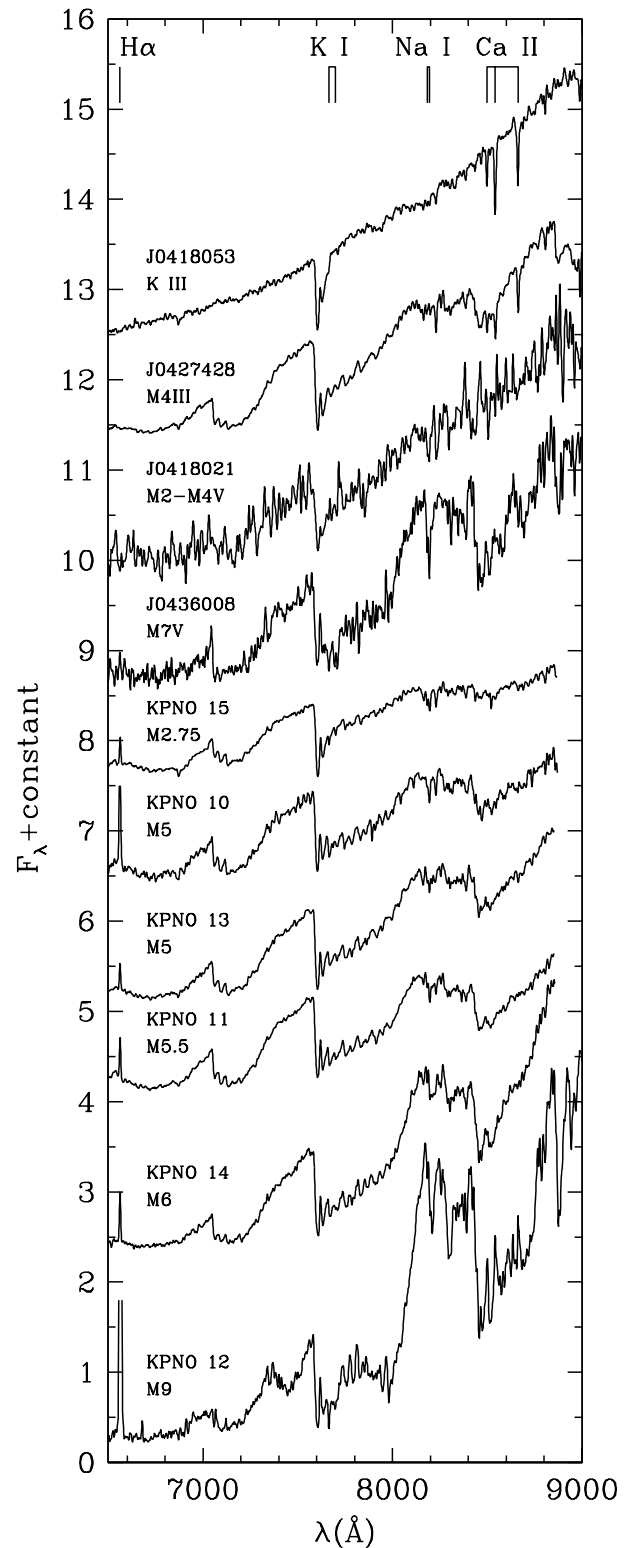


FIG. 2.—Spectra of candidate members of the Taurus star-forming region. The spectra of 2MASSs J0418053+282801 and J0427428+262256 exhibit the reddening and strong Ca II absorption that are expected of background field giants. The strong K I and Na I absorption in the data for 2MASSs J0436008+225517 is indicative of a field dwarf. Because this star and 2MASSs J0418021+281748 fall below the main sequence for the distance of Taurus and show significant reddening, they are probably background field dwarfs. The remaining six objects are confirmed as pre-main-sequence sources by the weak absorption in K I and Na I and strong emission in H α . All data are smoothed to a resolution of 8 Å and normalized at 7500 Å.

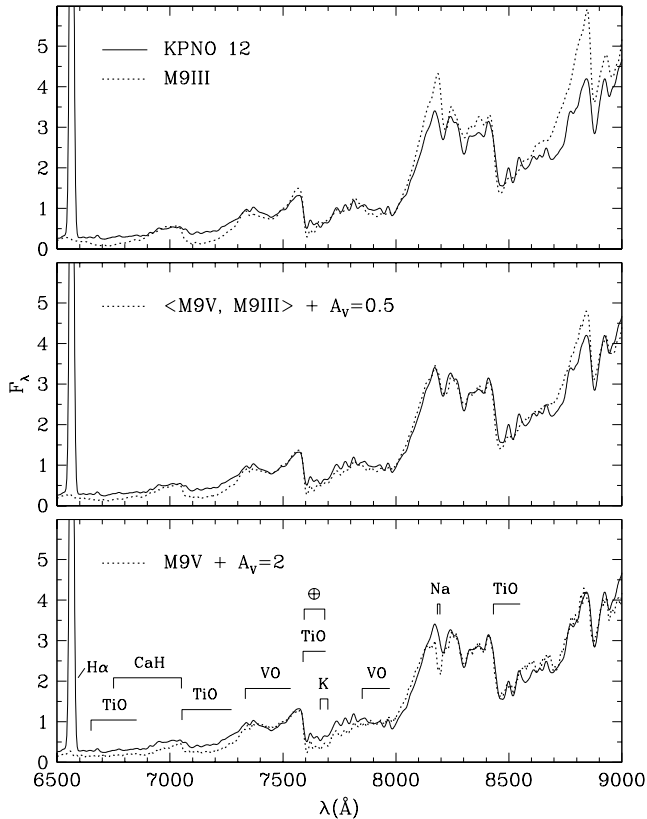


FIG. 3.—Spectrum of the new Taurus member KPNO–Tau 12 compared to data for M9 III, M9 V, and an average of the two types. Reddening is applied to the latter data to optimize the matches to the spectrum of KPNO–Tau 12. All data are smoothed to a resolution of 18 Å and normalized at 7500 Å.

that the best match to the optical spectrum is provided with an average of dwarf and giant spectra (normalized at 7500 Å), as shown in Figure 3, which is consistent with the results of our previous classifications of young objects later than M6 (Luhman 1999; Briceño et al. 2002). The spectrum for KPNO–Tau 12 in Figure 3 is from the November observations with Keck. We did not use the January data from the MMT in measuring the spectral type of this object because the signal-to-noise ratio (S/N) was too low.

The classifications and other measurements for the 16 background field stars and the six new Taurus members are listed in Tables 1 and 2, respectively. The photometric errors are ~ 0.1 mag for KPNO–Tau 12 and ~ 0.03 mag for the remaining sources.

5. PROPERTIES OF NEW MEMBERS

In this section, we use the photometry, spectroscopy, and theoretical evolutionary models to examine the physical properties of the six new Taurus members.

5.1. Disk and Accretion Signatures

Excess continuum emission and optical emission lines are signatures of circumstellar disks and accretion that could appear in the available data for the new Taurus members. The near-IR colors of the six new members match those of reddened dwarfs and have no significant excess emission in the *K* band. This is consistent with the observation that only

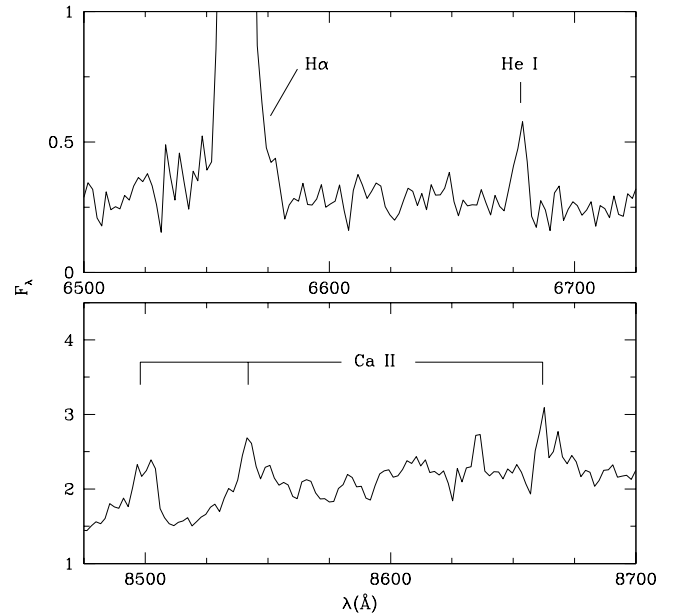


FIG. 4.—Emission lines in the spectrum of the new Taurus member KPNO–Tau 12. At a mass of $\sim 0.02 M_{\odot}$, this is the least massive object observed to date with He I and Ca II emission lines, which are typically found in stars undergoing intense accretion. These data have a resolution of 6 Å.

half of the known members of Taurus exhibit *K*-band excess emission, while a much larger fraction show evidence for disks in photometry at longer bandpasses such as *L* (Kenyon & Hartmann 1995; Haisch et al. 2000). Five of the new members show moderate to strong emission in $H\alpha$ ($W_{\lambda} = 6\text{--}36$ Å) that is typical of young stars in Taurus, while the M9 object KPNO–Tau 12 exhibits a far larger equivalent width. A given value of $L_{H\alpha}/L_{\text{bol}}$ corresponds to larger equivalent widths at later spectral types as the stellar continuum surrounding $H\alpha$ becomes weaker. In addition, when this faint continuum is detected at low S/N, it is possible to erroneously measure arbitrarily large values of the equivalent width. However, in the case of KPNO–Tau 12, the continuum near $H\alpha$ is well detected, as demonstrated in Figure 4. In measuring the equivalent width of $H\alpha$, the continuum level across the line was taken to be the level from the best-fit M9 standard (§ 4) after normalizing the two spectra at the surrounding continuum (6400–6500 and 6600–6700 Å). In this way, the equivalent width of $H\alpha$ is confidently measured to be between 850 and 1050 Å in the November spectrum. Because of insufficient S/N in the continuum surrounding $H\alpha$, an equivalent width was not measured from the January spectrum.

To compare the $H\alpha$ emission in KPNO–Tau 12 to that in other M-type sources, we consider the ratio $L_{H\alpha}/L_{\text{bol}}$. We arrived at two separate flux calibrations for the November spectrum of KPNO–Tau 12 by using the *I*-band photometry of this source from Briceño et al. (2002) and the data for the spectrophotometric standard. We adopted the average of these calibrations, which differed by 20%. From the resulting spectrum, we measured an $H\alpha$ flux of $(2.45 \pm 0.25) \times 10^{-15}$ ergs $\text{s}^{-1} \text{cm}^{-2}$ in the November data. Meanwhile, the flux of $H\alpha$ in the January spectrum was 30% higher. After correcting the November measurement for an extinction of $A_V = 0.5$ and combining the result with the bolometric luminosity derived in the next section, we find \log

$(L_{H\alpha}/L_{bol}) = -2.6 \pm 0.12$, which is slightly higher than the strongest emission observed in late M dwarfs (Schneider et al. 1991; Martín et al. 1999; Liebert et al. 1999) and 2 orders of magnitude greater than the typical values for these objects (Gizis et al. 2000). The only known young late M sources with comparable $H\alpha$ emission are LS-RCrA 1 in R Coronae Australis (Fernández & Comerón 2001) and S Ori 71 in σ Orionis (Barrado y Navascués et al. 2002). Several other young low-mass objects have been found with $H\alpha$ intensities that are only a few times lower than those in KPNO–Tau 12, LS-RCrA 1, and S Ori 71 (Zapatero Osorio et al. 2002; Briceño et al. 2002; Luhman et al. 2003).

There are additional indications that active accretion is probably occurring in KPNO–Tau 12. The TiO bands at 6600–7300 Å are weaker than those of the best-fit standard spectrum in Figure 3, which is suggestive of veiling from blue excess continuum emission. On the other hand, this behavior could imply a spectral type later than our classification of M9 since the TiO bands become weaker and eventually disappear from M to L types. But given the good quality of the fit of M9 to the data beyond 7300 Å and the presence of intense $H\alpha$ emission, the weak appearance of the TiO bands is probably a result of continuum veiling. We also detect emission in He I at 6678 Å and in the Ca II IR triplet, as shown in Figure 4. We measure equivalent widths of 8 ± 2 Å for He I and 4 ± 1 , 2.5 ± 1 , and 1.5 ± 0.5 Å for Ca II at 8498, 8542, and 8662 Å. KPNO–Tau 12 is the coolest young object known to exhibit these emission lines, which are usually indicators of intense accretion when observed in young stars (Muzerolle et al. 1998; Beristain et al. 2001).

Alternatively, emission in He I and Ca II, as well as strong $H\alpha$ and continuum veiling, can be attributed to a magnetic flare event, as in the case of the field M9.5 dwarf 2MASSW J0149090+295613 (Liebert et al. 1999). However, since the duty cycle of such flares is low in field objects (Gizis et al. 2000; Liebert et al. 2003) and the emission in KPNO–Tau 12 was strong at both epochs of our observations, the emission in KPNO–Tau 12 is probably not from a flare event. Given that KPNO–Tau 12 is member of a star-forming region, it is much more likely that the emission in $H\alpha$, He I, Ca II, and the blue continuum are the result of active accretion.

5.2. Extinctions, Temperatures, and Luminosities

Following the procedures described by Briceño et al. (2002), we estimate extinctions, effective temperatures, and bolometric luminosities from the spectral types and photometry for the six new Taurus members. The values for these parameters are listed in Table 2. The combined uncertainties in A_J , J , and BC_J ($\sigma \sim 0.14, 0.03, 0.1$) correspond to errors of ± 0.07 in the relative values of $\log L_{bol}$. When an uncertainty in the distance modulus is included ($\sigma \sim 0.2$), the total uncertainties are ± 0.11 . We use the temperatures and luminosities in Table 2 to place the six sources on the H-R diagram in Figure 5. For reference, we also show the previously known Taurus members that have $A_V \leq 4$ and are within the 8.4 deg² surveyed by Briceño et al. (1998, 2002) and Luhman (2000), which comprise the IMF sample from Briceño et al. (2002). The five new members at M3–M6 fall within this sequence of members, which is spread between less than 1 and 10 Myr for most masses. Meanwhile, the new M9 source KPNO–Tau 12 appears near the

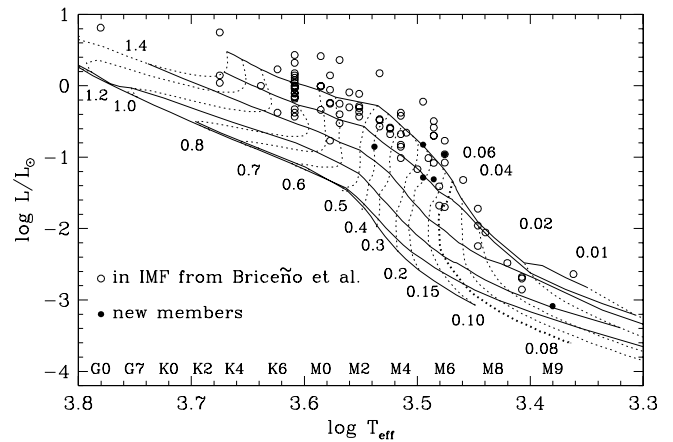


FIG. 5.—H-R diagram for young objects in the IMF for Taurus reported by Briceño et al. (2002, *open circles*). This sample is extinction-limited ($A_V \leq 4$) and applies to 8.4 deg² of Taurus surveyed by Briceño et al. (1998, 2002) and Luhman (2000). We have spectroscopically identified six new members in these fields (*filled circles*), which have $A_V \leq 4$ and thus are added to the IMF from Briceño et al. (2002) in Fig. 6. The theoretical evolutionary models of Baraffe et al. (1998) are shown, where the horizontal solid lines are isochrones representing ages of 1, 3, 10, 30, and 100 Myr and the main sequence, from top to bottom. The M spectral types have been converted to effective temperatures with a scale such that GG Tau Ba and Bb fall on the same model isochrone as Aa and Ab and that the M8–M9 members of Taurus and IC 348 have model ages that are similar to those of the earlier members (Luhman et al. 2003).

30 Myr model isochrone of Baraffe et al. (1998), as does one of the previously known M8.5 members. An age of 30 Myr is much larger than expected, given the median age of 1 Myr for the Taurus population and the apparent presence of active accretion in KPNO–Tau 12. Interestingly, the one other young late M source known to exhibit accretion signatures in the form of He I and Ca II emission, LS-RCrA 1, also falls much lower on the H-R diagram than expected (Fernández & Comerón 2001).

We consider three possible explanations for the anomalously old ages implied by the H-R diagrams of some late M sources, particularly KPNO–Tau 12 and LS-RCrA 1. First, there could be deficiencies in either the models or the conversion of spectral types to temperatures. In this work, we use a temperature scale that has been adjusted at late spectral types so that the low-mass members of Taurus and IC 348 have median ages comparable to the ones of the higher mass sources (Luhman et al. 2003). As a result, the adopted combination of models and temperature scale should produce the most reliable age and mass estimates that are currently possible. However, as suggested by Fernández & Comerón (2001) in the case of LS-RCrA 1, intense accretion could produce an evolutionary path on the H-R diagram that differs from that predicted by models of nonaccreting objects. Indeed, both of the known late M objects with evidence for accretion in the form of He I and Ca II emission are subluminal on the H-R diagram. Fernández & Comerón (2001) proposed a second explanation for the low luminosity of LS-RCrA 1 in which this object is seen in scattered light. For a young star that is occulted by an optically thick structure such as an edge-on disk, the observed photometry measures only the scattered light. As a result, the luminosity implied by the photometry is an underestimate, and the star appears subluminal for its temperature on the H-R diagram. For a low-mass source undergoing

intense accretion, it is possible that a significant fraction of the object is blocked by accreting circumstellar material, which could account for the correlation between accretion activity and low luminosity for KPNO–Tau 12 and LS–RCrA 1. However, this occulting mechanism would need to be more efficient for brown dwarfs than for stars since young stars in Taurus with He I emission do not have systematically lower luminosities than other stellar members. As a third possibility, the old ages inferred from the model isochrones could result from errors in the luminosity estimates of young sources. The finite width of the Taurus sequence on the H–R diagram could arise not from a spread in ages but from various sources such as extinction uncertainties, unresolved binaries, variability from accretion and from rotation of spotted surfaces, and differences in distances to individual members (Kenyon & Hartmann 1990; Hartmann 2001). If so, then the width of the sequence in $\log L$ should remain roughly constant at all masses, and thus correspond to an increasing apparent spread of ages as the separation between model isochrones in $\log L$ decreases from stellar to substellar masses. This phenomenon probably produces erroneously old ages on the model isochrones for at least some low-mass members of young clusters but would not explain the fact that both late-type objects showing He I emission are subluminal.

5.3. Masses

We now consider the masses of the new Taurus members. By combining the positions on the H–R diagram with the evolutionary models of Baraffe et al. (1998), we infer masses of 0.10, 0.13, 0.15, 0.16, and $0.4 M_{\odot}$ for KPNO–Tau 14, 11, 13, 10, and 15. These mass estimates are not sensitive to uncertainties in the luminosities since the predicted evolution of a star is mostly vertical on the H–R diagram for ages of less than 10 Myr. However, this is not true at substellar masses, where the mass tracks have significant components in both temperature and luminosity. The models imply a mass of $0.03 M_{\odot}$ for the M9 object KPNO–Tau 12 based on its position on the H–R diagram. Under two of the three explanations for the low luminosity of this source (§ 5.2), the luminosity estimate is uncertain. In these cases, a more reliable mass is derived by placing the object on the 1 Myr isochrone for the adopted temperature, which would imply a mass of $0.015 M_{\odot}$ from the models of Baraffe et al. (1998). For the third explanation in which the temperature and luminosity are significantly affected by accretion, KPNO–Tau 12 could have an even lower mass (Fernández & Comerón 2001). If this object does have a mass below $0.015 M_{\odot}$, one might be tempted to refer to it as an accreting free-floating planetary mass object. However, the various properties of low-mass brown dwarfs—such as the evidence of intense accretion in objects like KPNO–Tau 12—indicate that they probably form in a starlike fashion rather than in circumstellar disks (Briceño et al. 2002). Therefore, the term “planetary” has little or no applicability. For the purposes of this work, we adopt a mass of $0.02 M_{\odot}$ for this object.

As mentioned previously, the IMF presented by Briceño et al. (2002) included the 86 known Taurus members that fell within the 8.4 deg^2 surveyed by Briceño et al. (1998, 2002) and Luhman (2000) and that had extinctions of $A_V \leq 4$. There remained a few potential members that lacked spectroscopy within these defining parameters, so the IMF sample was not 100% complete. However, because

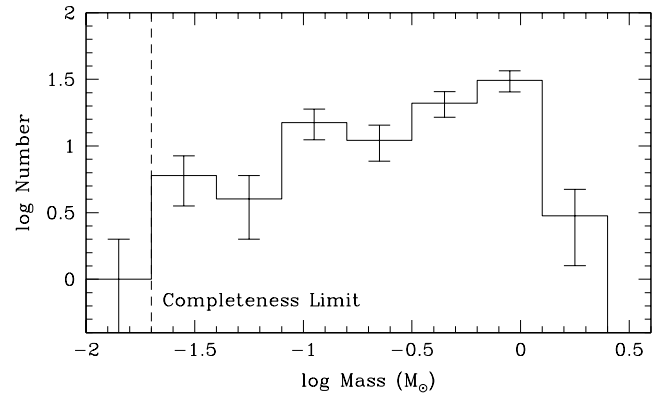


FIG. 6.—IMF for an extinction-limited sample ($A_V \leq 4$) of young objects in the 8.4 deg^2 of Taurus surveyed by Briceño et al. (1998, 2002) and Luhman (2000). This sample consists of the 86 Taurus members in the IMF from Briceño et al. (2002) and the six new members found in this work. In the units of this diagram, the Salpeter slope is 1.35.

the candidates were not concentrated at a particular magnitude range, Briceño et al. (2002) concluded that the sample of confirmed members was unbiased in mass down to the completeness limit of the photometry, which corresponded to $0.02 M_{\odot}$ for $A_V = 4$. Through spectroscopy of those candidates, we have found six new members, all of which have $A \leq 4$. After adding these sources to the extinction-limited sample from Briceño et al. (2002), we arrive at the IMF in Figure 6, which should be virtually 100% complete for $A_V \leq 4$ and masses above $0.02 M_{\odot}$ in the 8.4 deg^2 survey fields. Because of the small number of new members that are added to the IMF from Briceño et al. (2002) and the wide range of masses of these new sources, the shapes of the IMFs here and in Briceño et al. (2002) do not differ significantly. Thus, the conclusions from Briceño et al. (2002) regarding the observed variations in the IMFs of Taurus and the Trapezium remain unchanged.

6. CONCLUSIONS

We have obtained spectroscopy for candidate young stars and brown dwarfs that appeared in an optical and IR photometric survey of 8 deg^2 of the Taurus star-forming region by Briceño et al. (2002). We have estimated individual extinctions for the stars detected in the survey and have plotted the dereddened photometry on color-magnitude diagrams. Within an extinction limit of $A_V \leq 8$, we identified 22 sources that were potential members of Taurus and that lacked previous spectroscopy. Through optical spectroscopy of these candidates, we have discovered six new members with spectral types ranging from M2.75 to M9. From the spectral types and photometry of these objects, we have estimated extinctions, effective temperatures, and bolometric luminosities, and have combined these results with the evolutionary models of Baraffe et al. (1998) to infer individual masses that range from 0.4 to $0.02 M_{\odot}$. These new members fall within the extinction limit of $A_V \leq 4$ that defined the sample from which Briceño et al. (2002) derived an IMF. Therefore, we have added them to that extinction-limited sample and have presented the updated IMF, which applies to the 8.4 deg^2 in Taurus surveyed by Briceño et al. (1998, 2002) and Luhman (2000). The new M9 source is a particularly interesting discovery from this work. It has the

second latest spectral type of the known members of Taurus. In addition, it exhibits the strongest $H\alpha$ emission observed to date for a late M source [$W_\lambda \sim 950 \text{ \AA}$, $\log(L_{H\alpha}/L_{\text{bol}}) = -2.6$] and is the least massive object found with emission in He I 6678 \AA and the Ca II IR triplet, which are suggestive of active accretion. High-resolution spectroscopy of the emission lines in this object would provide valuable insight into the formation of low-mass brown dwarfs.

We thank Perry Berlind and Mike Calkins for performing the FAST observations. K. L. was supported by grant NAG5-11627 from the NASA Long-Term Space Astrophysics program. C. B. received partial support from grant S1-2001001144 of the Fondo Nacional de Ciencia y Tecnología (FONACYT) of Venezuela. We are grateful to France Allard and Isabelle Baraffe for access to their most recent calculations. This research has made use of the NASA/

IPAC Infrared Science Archive, which is operated by the Jet Propulsion Laboratory, California Institute of Technology, under contract with the National Aeronautics and Space Administration. Some of the data presented herein were obtained at the W. M. Keck Observatory, which is operated as a scientific partnership among the California Institute of Technology, the University of California, and the National Aeronautics and Space Administration. The Observatory was made possible by the generous financial support of the W. M. Keck Foundation. We wish to extend special thanks to those of Hawaiian ancestry on whose sacred mountain we are privileged to be guests. Without their generous hospitality, some of the observations presented herein would not have been possible. Some of the data in this work were obtained at the MMT Observatory, a joint facility of the Smithsonian Institution and the University of Arizona.

REFERENCES

- Baraffe, I., Chabrier, G., Allard, F., & Hauschildt, P. H. 1998, *A&A*, 337, 403
- Barrado y Navascués, D., Zapatero Osorio, M. R., Martín, E. L., Béjar, V. J. S., Rebolo, R., & Mundt, R. 2002, *A&A*, 393, L85
- Beristain, G., Edwards, S., & Kwan, J. 2001, *ApJ*, 551, 1037
- Briceño, C., Hartmann, L., Stauffer, J., & Martín, E. L. 1998, *AJ*, 115, 2074
- Briceño, C., Luhman, K. L., Hartmann, L., Stauffer, J. R., & Kirkpatrick, J. D. 2002, *ApJ*, 580, 317
- Fabricant, D., Cheimets, P., Caldwell, N., & Geary, J. 1998, *PASP*, 110, 79
- Fernández, M., & Comerón, F. 2001, *A&A*, 380, 264
- Gizis, J. E., Monet, D. G., Reid, I. N., Kirkpatrick, J. D., Liebert, J., & Williams, R. J. 2000, *AJ*, 120, 1085
- Haisch, K. E., Lada, E. A., & Lada, C. J. 2000, *AJ*, 120, 1396
- Hartmann, L. 2001, *AJ*, 121, 1030
- Kenyon, S. J., & Hartmann, L. 1990, *ApJ*, 349, 197
- . 1995, *ApJS*, 101, 117
- Leggett, S. K. 1992, *ApJS*, 82, 351
- Liebert, J., Kirkpatrick, J. D., Cruz, K. L., Reid, I. N., Burgasser, A., Tinney, C. G., & Gizis, J. E. 2003, *AJ*, 125, 343
- Liebert, J., Kirkpatrick, J. D., Reid, I. N., & Fisher, M. 1999, *ApJ*, 519, 345
- Luhman, K. L. 1999, *ApJ*, 525, 466
- Luhman, K. L. 2000, *ApJ*, 544, 1044
- Luhman, K. L., Briceño, C., Rieke, G. H., & Hartmann, L. W. 1998a, *ApJ*, 493, 909
- Luhman, K. L., & Rieke, G. H. 1998, *ApJ*, 497, 354
- Luhman, K. L., Rieke, G. H., Lada, C. J., & Lada, E. A. 1998b, *ApJ*, 508, 347
- Luhman, K. L., et al. 2003, *ApJ*, submitted
- Martín, E. L., Basri, G., & Zapatero Osorio, M. R. 1999, *AJ*, 118, 1005
- Martín, E. L., Dougados, C., Magnier, E., Ménard, F., Magazzù, A., Cuilandre, J.-C., & Delfosse, X. 2001, *ApJ*, 561, L195
- Martín, E. L., Rebolo, R., & Zapatero Osorio, M. R. 1996, *ApJ*, 469, 706
- Muzerolle, J., Hartmann, L., & Calvet, N. 1998, *AJ*, 116, 455
- Oke, J. B., et al. 1995, *PASP*, 107, 375
- Schneider, D. P., Greenstein, J. L., Schmidt, M., & Gunn, J. E. 1991, *AJ*, 102, 1180
- Strom, K. M., & Strom, S. E. 1994, *ApJ*, 424, 237
- Wichmann, R., Bastian, U., Krautter, J., Jankovics, I., & Ruciński, S. M. 1998, *MNRAS*, 301, L39
- Zapatero Osorio, M. R., Béjar, V. J. S., Martín, E. L., Barrado y Navascués, D., & Rebolo, R. 2002, *ApJ*, 569, L99